© IIJP 2026 | Volume 2, Issue 1, pp. 854-866 | ISSN: 2636-4484

GREEN SYNTHESIS OF COPPER OXIDE NANOPARTICLES USING *CARICA PAPAYA* LEAF EXTRACT FOR ADSORPTIVE REMOVAL OF WATER HARDNESS

Umar Ibrahim[1], Sa' adatu Eri Mohammed[2], Aminu Bala[3], Ibrahim Bala Ata[4], Abubakar Shehu[5] & Sabiu Alhassan[6]

[1,2,3]Department of Chemistry, Federal University Dutse, Jigawa State, Nigeria.

[4]Laboratory Unit, Faculty of Physical sciences, Federal University Dutse, Jigawa State, Nigeria.

[5]Department of Community Health, Jigawa State Polytechnic, Dutse, Jigawa State, Nigeria.

[6]Department of Chemistry, Nigeria Police Academy Wudil, Kano State Nigeria

Corresponding author: Umar Ibrahim - Uibrahim997@gmail.com/+2347070763175

ARTICLE INFO

Article No.: 0191

Accepted Date: 03/02/2026

Published Date: 28/02/2026

Type: Research

ABSTRACT

Water hardness, primarily driven by divalent cations such as Ca^{2+} and Mg^{2+}, poses significant technical and economic challenges for both domestic and industrial sectors. Traditional remediation techniques are often limited by high operational costs and adverse environmental impacts. This study investigates the green synthesis of copper oxide (CuO) nanoparticles as a sustainable and cost-effective adsorbent for water softening. The synthesized nanoparticles were characterized using X-ray diffraction (XRD), which confirmed a crystalline structure with an average crystallite size of 9.6 nm (Scherrer equation), and Fourier-transform infrared (FTIR) spectroscopy, which validated the presence of functional groups and CuO phase through characteristic vibrational modes. Scanning electron microscopy (SEM) further revealed the surface morphology and particle distribution of the adsorbents. Batch adsorption experiments were conducted on real-world water samples, demonstrating a reduction in total hardness from an initial 174 mg/L to 40 mg/L. Under optimized conditions, the CuO nanoparticles achieved a maximum removal efficiency of 77%. The adsorption mechanism suggests that the high surface-area-to-volume ratio facilitates rapid sequestration of Ca^{2+} and Mg^{2+} ions via surface complexation or ion exchange. These results indicate that plant-mediated CuO nanoparticles represent a viable, eco-friendly, and high-performance alternative for advanced water purification.

Keywords: Green synthesis, CuO nanoparticles, Carica papaya, Adsorption, Water hardness Removal, Complexometric titration

Introduction

Over the last two decades, the synthesis and application of nanoparticles (NPs) have become a prominent area of scientific research. Due to their unique physical and chemical properties, NPs are now essential in various fields, including animal feed, environmental remediation, and medicine (Moroda *et al.,* 2025). Copper nanoparticles (Cu NPs) are particularly versatile, serving as effective antimicrobial, antitumor, and antioxidant agents, as well as catalysts for the decomposition of substances and color removal.

However, synthesizing Cu NPs through conventional chemical methods presents several disadvantages. These methods can be difficult to execute and hazardous because they utilize toxic chemicals such as hydrazine, N-dimethylformamide, and sodium borohydride which are associated with health risks, including cancer (Kalaiyan *et al.,* 2025).

To mitigate these issues, plant-based synthesis has emerged as a superior method for reducing and stabilizing metal ions (Manimehala *et al.,* 2025). By utilizing natural extracts as reducing and stabilizing agents, these biosynthetic techniques offer an affordable, simple, and eco-friendly alternative. While microorganisms can facilitate intracellular or extracellular synthesis (Baral *et al.,* 2025), using plant extracts remains a cost-effective and sustainable approach to nanoparticle production.

Water hardness occurs when soap fails to lather effectively, primarily due to the presence of dissolved metallic cations with multiple positive charges. Calcium (Ca^{2+}) and magnesium (Mg^{2+}) are the primary contributors, though other ions such as strontium (Sr^{2+}), barium (Ba^{2+}), iron (Fe^{2+}), and zinc (Zn^{2+}) also contribute (Swarna *et al.,* 2025). Total hardness is measured by the combined concentrations of Ca^{2+} and Mg^{2+}, expressed as mg/L of $CaCO_3$.

Calcium and magnesium are ubiquitous in natural water, ranking as the fifth and eighth most abundant elements, respectively. Their concentrations vary significantly from a few to several hundred mg/L depending on the water source and treatment processes (Boddu *et al.,* 2025). While humans can typically taste calcium in drinking water at levels between 100 and 300 mg/L, higher concentrations may be tolerated. Consequently, frequent water quality monitoring, particularly for total hardness, is vital for both industrial applications and drinking water plants. EDTA titrimetric methods remain the standard protocol for these assessments.

Despite the global shift toward green synthesis, there is a significant lack of empirical data regarding the optimization of *Carica papaya*-mediated CuO nanoparticles specifically tailored for complex aqueous matrices. Current literature focuses heavily on synthetic solutions, leaving a critical research gap in how these nanoparticles interact with the unique chemical profiles of naturally hard water sources in Northern Nigeria. Furthermore, the mechanism of ion-exchange and surface complexation between *Carica papaya* functionalized CuO and divalent cations (Ca^{2+}, Mg^{2+}) in these specific environmental conditions has not been fully elucidated.

Materials and Methods

Reagent and Equipment

The research utilized analytical-grade reagents. These have a high standard of purity (typically ≥ 95%), ensuring that the results are not skewed by significant impurities. Reagents included copper (II) sulfate ($CuSO_4$), potassium hydroxide (KOH), sodium hydroxide (NaOH), and hydrochloric acid (HCl), which were purchased from Sigma-Aldrich. Stock solutions were prepared using deionized water to ensure minimal ionic interference. The $CuSO_4$ solution was prepared at concentration of 2.0 M by dissolving 49.9 g of $CuSO_4$. $5H_2O$ in 1000 m L of water. Standardized solution of NaOH and KOH (2.0 M) were prepared by dissolving 80.00 g and 11.22 g of their respective pellets in 1 L of deionized water. All volumetric measurements were

performed using calibrated titration assemblies at room temperature. Experimental procedures were supported by standard laboratory instrumentation, specifically a pH meter, analytical balance, furnace, oven, and a magnetic hot plate stirrer. The experiment also used additional tools which included a thermometer, as well as titration assemblies.

Methods

Preparation of Extract

To prepare the extract, fresh leaves were rinsed using distilled water and kept to dry in the shade at 25-30 ^{0}C for one week. The completely dried leaves were then ground so as to form a fine powder. An aqueous extract was prepared by heating 6 g of the powder in 100 mL of distilled water at 60 0C for one hour during which constant stirring was maintained. The solution was cooled, passed through Whatman No. 1 filter paper, and the resulting filtrate was stored at 4 ^{0}C for subsequent usage (Gaddigal *et al.,* 2025). Choudhary *et al.* (2025) confirmed the presence of several phytochemicals in *papaya* leaves, including alkaloids, flavonoid, phenolic compounds, saponins, tannins, terpenoids, and glycosides

Preparation of 0.01 M EDTA

Approximately 3.722 g of the EDTA disodium salt was accurately weighed using an analytical balance. The salt was transferred onto a 1000 mL volumetric flask, and approximately 600 mL of distilled water was added with constant stirring until the crystals are completely dissolved and the solution was clear. The flask was then filled with distilled water until the bottom of the meniscus touched the calibration mark.

Titration Procedure for Water Hardness

The standard reference for measuring water hardness is method 2340 from the standard methods for the examination of water and wastewater; published by the APHA (American Public Health Association). The titration process was commenced by pipetting 50 mL of the sample water and moved into a conical flask. To ensure the right pH for the reaction, 2 mL of pH buffer solution was measured and added to the flask. A tiny amount of the indicator, Eriochrome Black T (EBT), was also introduced. The burette was filled with the standardized chelating liquid, EDTA (ethylendiaminetetraacetic acid) (Ezeoke *et al.,* 2025).

The EDTA was gradually added drop-wise into the conical flask from the burette, with the flask contents being shaken consistently. The end of the titration exercise was marked by a distinct color change in the solution, from wine-red to a clear blue. To ensure precision and get an average volume of EDTA used, the whole procedure underwent three repeats (Kalesh and Vadhavaniya, 2025).

Plant-Based Synthesis of Copper Oxide Nanoparticles

The preparation followed the methodology done by Ge *et al.* (2025) with small tweaks to the original protocol. Equal divisions (50 mL each) of plant extract and 0.2 M copper sulfate ($CuSO_4$) solution were put together. The solution continuously underwent stirring at 60 ^{0}C which lasted for 15 minutes. The resulting solid was isolation using centrifugation, to get rid of impurities. The precipitate was washing three times with distilled water. The purified product was kept to dry in an oven at 50 ^{0}C for a period of 24 hours.

Characterization Techniques

Various physicochemical methods were employed to verify the successful synthesis of copper oxide nanoparticles.

UV-Vis Spectroscopy

UV–Vis spectra underwent recording between 200–800 nm (Motras Scientific UV Plus spectrophotometer).

Fourier-Transform Infrared Spectroscopy

For the fourier transform infrared spectroscopy FTIR analysis (400–4000 cm^{-1}) was performed using KBr pellets on a Perkin Elmer Spectrum Two instrument.

X-Ray Diffraction

XRD patterns were obtained on a Rigaku MiniFlex II diffractometer (Cu-Kα radiation, λ = 0.154 nm, 2θ = 20–80°), with crystallite size estimated via the Debye-Scherrer formula and phase identification against JCPDS database (Joint Committee on Powder Diffraction Standards) database and International Centre for Diffraction Data (ICCD).

X-Ray Spectroscopy

The morphology to determine shape lattice and chemical composition of synthesized nanoparticles were examined by scanning electron microscope (SEM; Model No. JSM 6510LV, Make-JEOL, Japan) equipped with energy dispersive X-ray spectrometer (EDSX) followed by microscopic imaging performed from 1000X to 30,000X with 0.5–1μm resolution at15kV.

Batch Adsorption Experiments

The natural polluted water (100 mL) was measured and transferred into five conical flasks and varying doses (100 mg L^{-1} – 500 mg L^{-1}) were measured and transferred into each flask. The different mixtures obtained were filtered and the filtrate was titrates for Ca^{2+} and Mg^{2+} using EDTA method (Abdelmonem *et al.,* 2025).

Result and Discussion

UV-Vis Spectroscopic Analysis

This study puts emphasis on rapid and lasting synthesis of copper oxide nanoparticles using *carica papaya* extract. Many works of literature suggests that *carica papaya* leaves are rich in bioactive compounds, including triterpenes, alkaloids, steroids, and phenols (Rogóż *et al.,* 2025). In this study, the synthesis mechanism can be linked to the phenolic content within the extract, which possesses the ability of a reducing agent (Singh *et al.,* 2025). Specifically, gallic acid which forms a primary phenolic component in the extract likely plays a part in reducing $Cu(OH)_2$ into nano-sized CuO (Joolaei Ahranjani *et al.,* 2025). As the pH was adjusted to 8.0, a color transition from blue to brown and finally to black was clearly seen. UV-Vis absorption spectra which underwent recording between 200-800 nm showed a dual peak at 204 nm and 214 nm, which affirm the creation of CuO NPs in agreement with previously documented data (Figure 1).

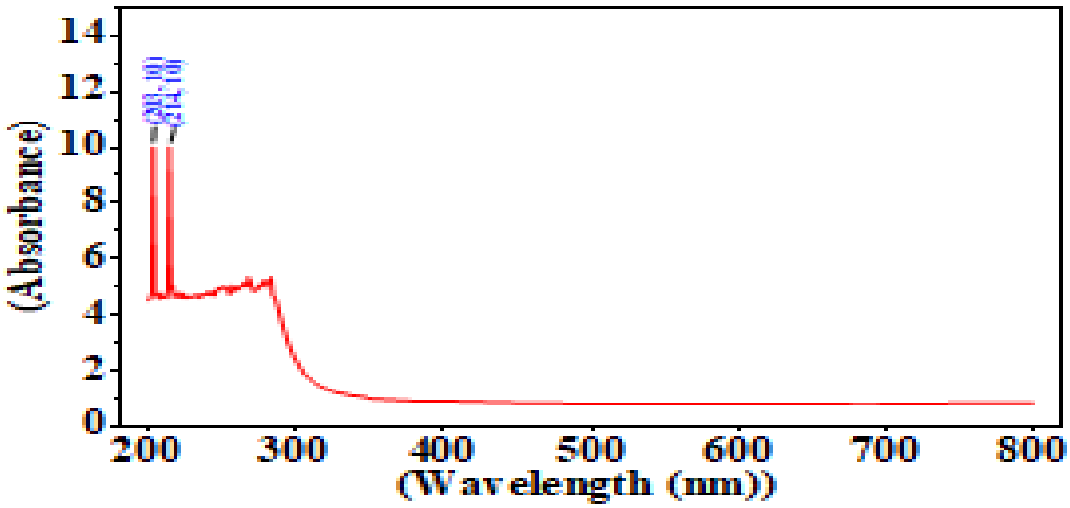

Figure 1: UV-visible spectroscopy

FTIR Analysis

The FTIR spectra for the synthesized CuO NPs showed some distinct absorption bands within the ranges of 3400-3500 cm^{-1}, 2800-3000 cm^{-1}, 1500-1700 cm^{-1}, and 1000-1300 cm^{-1}. A broad signal spotted at 3257 cm^{-1} can be linked to the vibrations arising from phenolic constituents in the solution. A minor peak at 2900 cm^{-1} suggests C-H bond stretching, while a sharp peak spotted at 1648 cm^{-1} suggests the existence of C=N or C=O functional groups. The bond detection at 1077 cm^{-1}, together with the OH signal, attests to the presence of C-O bonds which are associated with carbohydrates, hence, improving the stability of the nanoparticles. In conclusion, a characteristic sharp peak spotted at 590.4 cm^{-1} backs up the findings by Alfaifi *et al.* (2025)

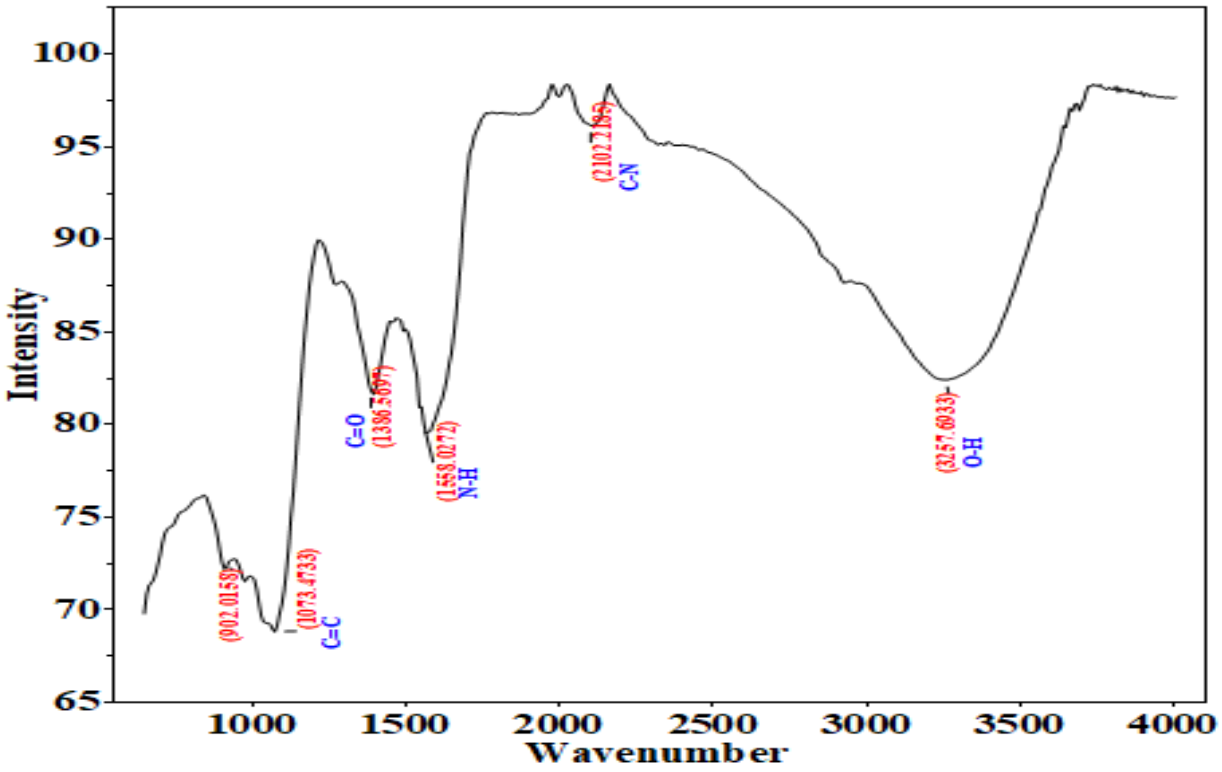

Figure 2: FTIR analysis

XRD Analysis

The XRD pattern of the biosynthesized CuO nanoparticles is displayed in Figure 3 below. The product possesses a pure and crystalline structure, as seen by the samples diffraction pattern matching the hexagonal CuO standard X-ray diffraction peaks JCPDS 00-36-1451. The reflections denoted by the XRD peaks noted at 31.99, 34.50, 36.33, 47.55, 56.55, 62.81, and 67.97 theta values correlate with the lattice plane (100), (002), (101), (102), (110), (103), and (112), respectively. Similar XRD findings for CuO nanoparticles were also published in previos lstudies (Veg *et al.,* 2025). However, based on the Scherrer's equation, the mean crystallite size of the generated CuO NPs was calculated as 9.6 nm as indicated by the lattice characteristics.

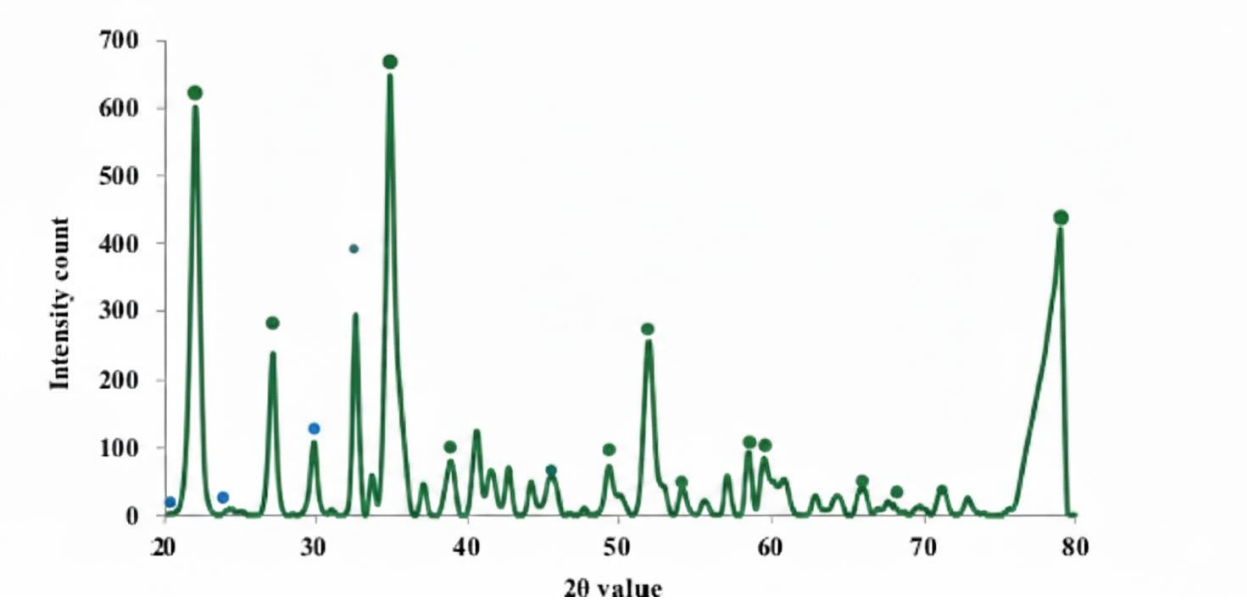

Figure 3: X-ray diffraction pattern of CuO NPs

SEM/EDX Analysis

Scanning Electron Microscopic SEM analysis indicates that particles more specifically consist of particles that are usually irregularly shaped, instead of those that assume the shape of highly spherical or fibrous structures. The particles possess sharp edges and facets, hence hinting that it is not spherical, angular, or fractured in morphology (Figure 4). The different samples display wide-ranging particle sizes, which imply that they are polydisperse. There are extremely minute fines that are visible between the larger particles. Selim *et al.* (2025) report similar results using mint leaves for the synthesis of copper oxide nanoparticles.

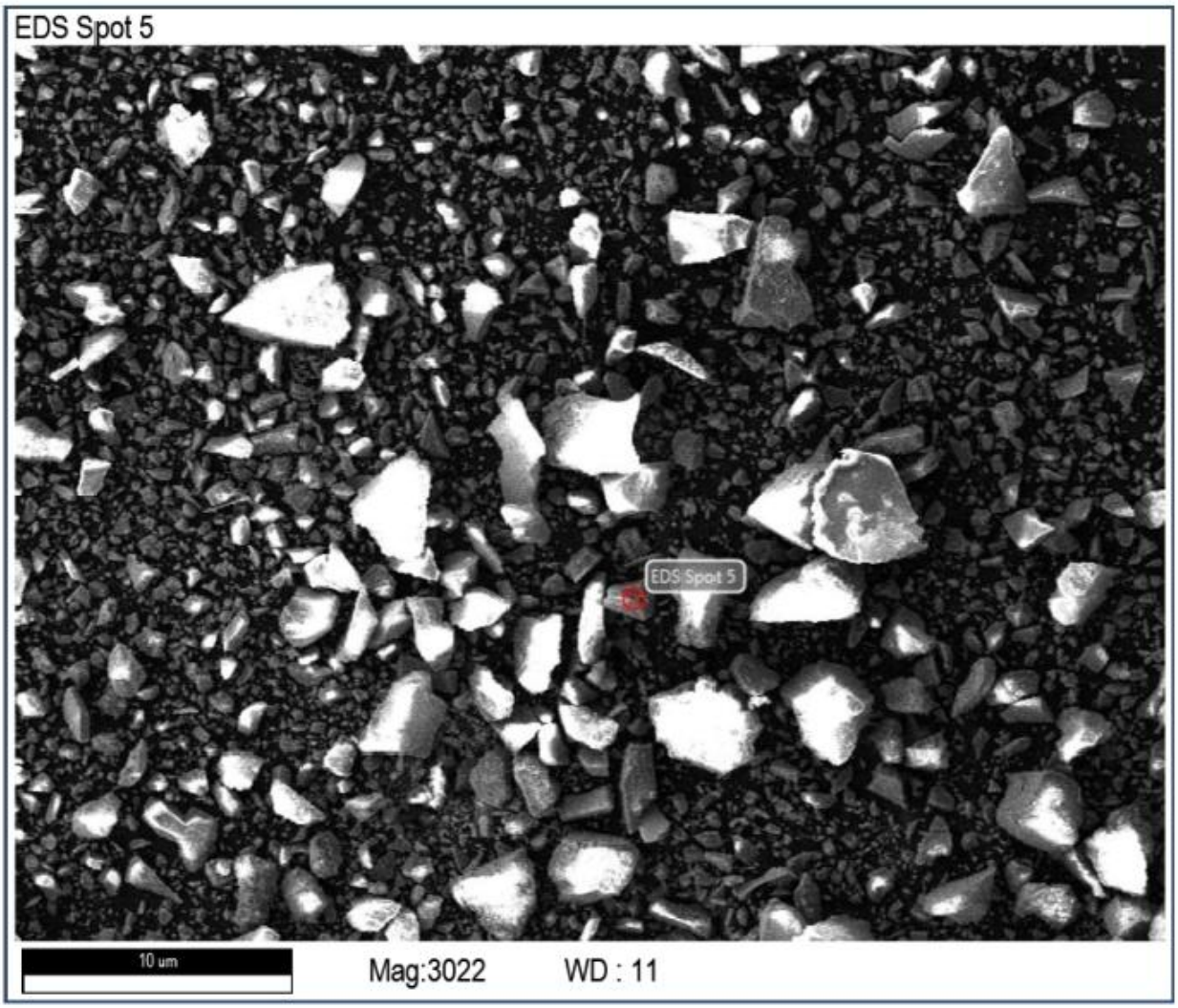

Figure 4: SEM analysis

The EDX spectroscopy was used to measure the elemental composition of synthesized nanoparticles. The spectrum of CuO NPs is shown in figure 5, which attests to the existence of Cu, O and C. The peak which is around 0.5 keV is indicative of a binding energy of oxygen (OKα); while peaks spotted at emission energies of 1, 8 and 9keV correspond to CuLα, CuKα, and CuKβ, in that order. In addition, a peak spotted at 0.25 keV corresponding to carbon (CKα) was also recorded. The percentage of Cu, O, and C contained in CuO NPs was found to be 17.51%, 42.49%, and 48.69% respectively. This heterogeneity contrasts with the more uniform EDX profiles observed in chemical syntheses but agrees with green methods which makes use of tea extracts (Hadkar and Selvaraj, 2025). The existing alkali metals could be from plant minerals, thereby improving biocompatibility.

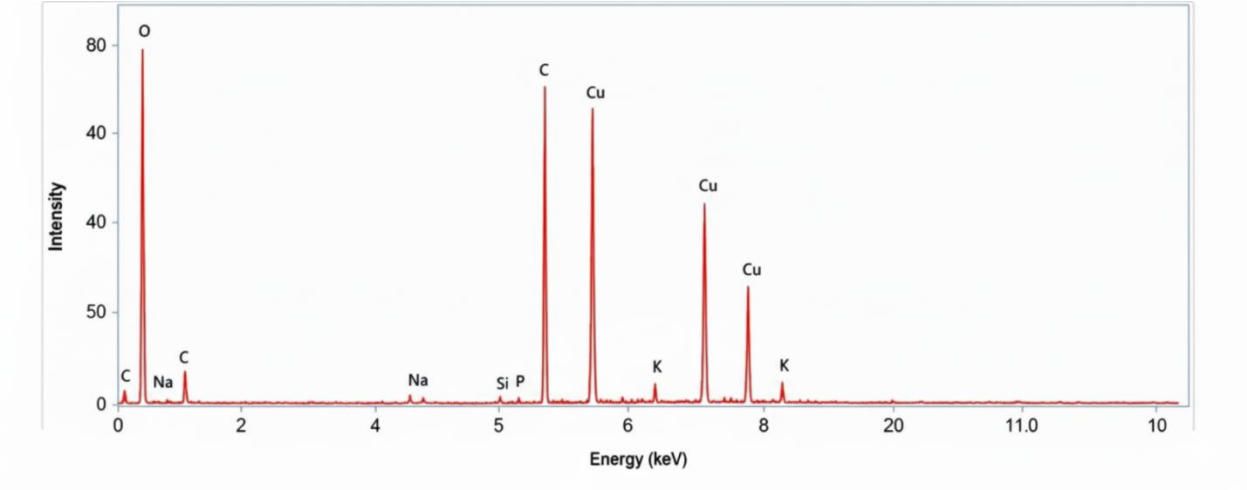

Figure 5: EDS analysis

Discussion of Findings

An interesting finding was observed regarding the Surface Plasmon Resonance (SPR) of the synthesized nanoparticles. While the characteristic SPR for CuO nanoparticles is typically reported between 250 nm and 300 nm (Sankar *et al.,* 2014), or occasionally up to 350 nm, these peaks are often associated with the phenolic capping agents (such as gallic acid) themselves. This suggests the initial formation of very small, quantum-confined copper-based clusters before they aggregate into larger nanoparticles (NPs). The dual-mode interaction between the *Carica papaya* bio-extract and copper ions during the nucleation phase aligns with Singh *et al.* (2025), who noted that phytochemicals like phenols and flavonoids act as primary antioxidants. Specifically, gallic acid facilitates the reduction of Cu^{2+} ions to CuO (Joolaei Ahranjani *et al.,* 2025). Similar studies using *Carica papaya* (e.g., Sankar *et al.,* 2014) confirm that the high antioxidant content of the leaves is responsible for the rapid stabilization of the NPs.

The FTIR spectra of the biosynthesized CuO NPs reveal various functional groups acting as reducing and stabilizing agents. A broad, intense absorption band at 3257 cm^{-1} is attributed to hydroxyl groups and alcohols present in the botanical extract, which facilitate the reduction of copper ions. This observation is consistent with Elango *et al.* (2025), who reported similar hydroxyl clusters in the synthesis of metal oxides.

Furthermore, the minor peak at 2900 cm^{-1} corresponds to the asymmetric C-H stretching of aliphatic groups, while the sharp peak at 1648 cm^{-1} is characteristic of C=O stretching (Amide I) or aromatic vibrations. Biomolecules from the extract are clearly involved in the capping process to prevent nanoparticle agglomeration. This aligns with Alfaifi *et al. (*2025), who identified these nitrogen-containing functional groups as critical for NP stabilization. According to Deepa *et al.* (2025), these biomolecules contribute significantly to the long-term stability and biocompatibility of the nanoparticles.

Significantly, the characteristic sharp peak at 590.4 cm^{-1} confirms the formation of the monoclinic phase of CuO. This position aligns with structural data reported by Alfaifi *et al.* (2025) and Sridharan *et al.* (2025) for high-purity copper oxide nanostructures. Regarding elemental ratio variance, the peak positions are scientifically accurate: the presence of the Carbon peak at ~0.25 keV, Oxygen at ~0.5 keV, and Copper peaks at 1 keV, 8 keV, and 9 keV (corresponding to CK_α, OK_α, CuL_α, and CuK_α matches recent nanoparticle characterizations (Aksel *et al.,* 2023).

Water Hardness Removal Using Copper Oxide Nanoparticles (CuO NPs)

Hardness in water is due to the presence of dissolved salts of calcium and magnesium. The estimation of hardness is based on complexometric titration. The hardness of water is determined by titrating with a standard solution of ethylenediaminetetraacetic acid (EDTA), which is the complexing agent. The hard water treatment with CuO NPs at different concentrations is depicted in Table 1. The initial concentration of hardness for the collected water samples is 174 mg L^{-1}. After treatment with CuO NPs, there is a clear positive correlation between the dose of CuO NPs and the removal efficiency. As dosage increases from 100 mg L^{-1} to 500 mg L^{-1}, the hardness removed increases steadily from 74 mg L^{-1} to 134 mg L^{-1}. This suggests the nanoparticles provide active surface sites for the adsorption of hardness-causing ions (Ca^{2+} and Mg^{2+}). More nanoparticles mean more surface area available for these ions to bind to. The initial hardness of 174 mg L^{-1} is generally classified as hard water. At the highest dose (500 mg L^{-1}), the final concentration drops to 40 mg L^{-1}. This effectively shifts the water from hard to soft. This suggests that CuO NPs have a high surface-area-to-volume ratio, allowing them to attract and hold divalent cations (Ca^{2+}, Mg^{2+}) on their surface through electrostatic or chemical bonding.

The sample shows the best compatibility with this treatment. While efficiency increases with dosage, the rate of increase often slows down as the dose gets higher. In the sample the jump from 100 to 200 mg L^{-1} improved efficiency by 15%. The jump from 400 to 500 mg L^{-1} only improved efficiency by 9.2%. Furthermore, our hardness reduction (up to 77% at 500 mg/L) is promising, though literature regarding the use of CuO for Ca^{2+} and Mg^{2+} removal remains sparse. These results are consistent with findings for carbon nanoparticles derived from *Phyllanthus emblica,* which also reduce hardness via adsorption.

Table 1: Summary of Hardness Removal using (CuO NPs- A)

Dose of CuO NPs (mg L^{-1})	Final concentration (mg L^{-1})	Hardness removed (mg L^{-1})	Removal Efficiency (%)
100	100	74	42.5
200	74	100	57.5
300	66	108	62.1
400	56	118	67.8
500	40	134	77.0

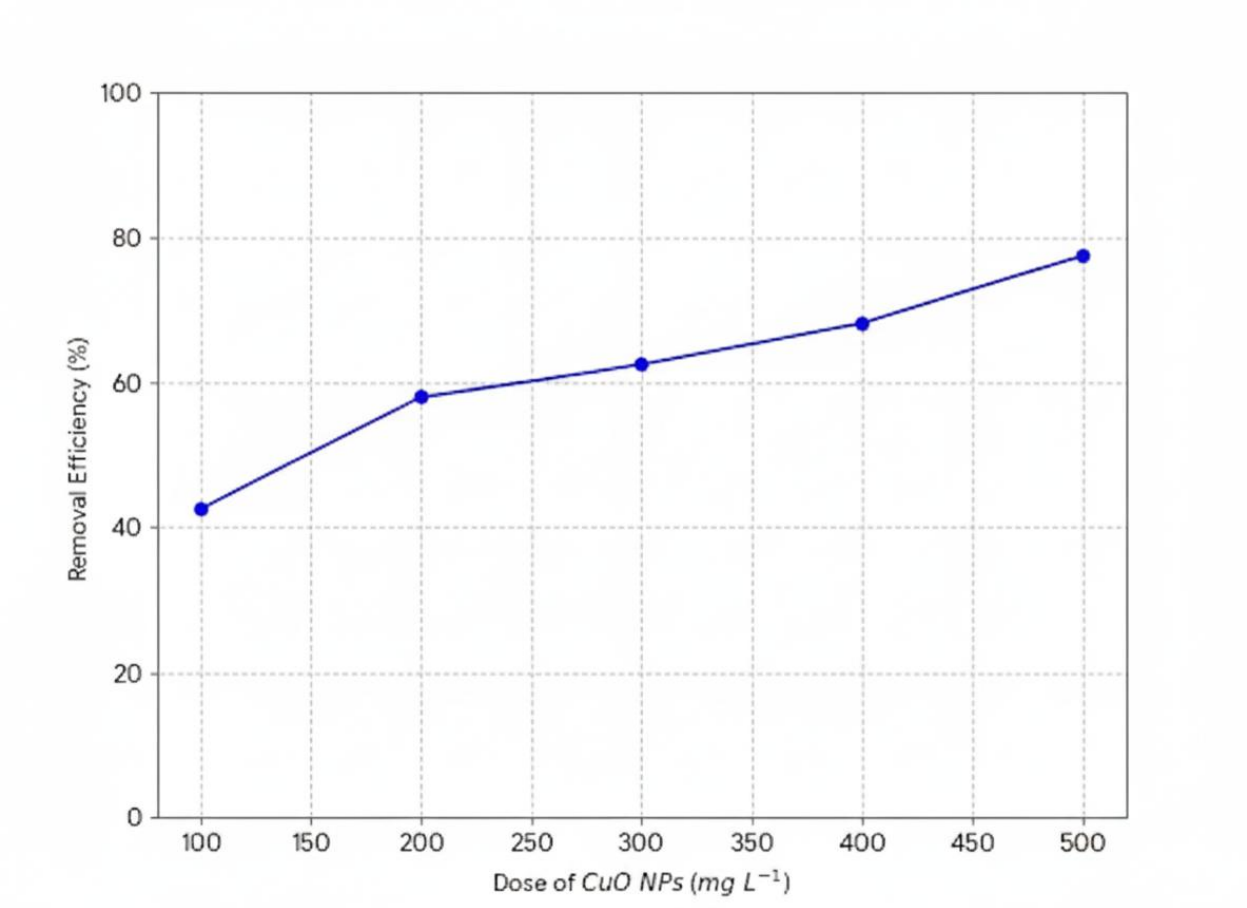

Figure 6: Effect of Adsorbent Dose on Removal of Hardness

Conclusion

This study successfully synthesized copper oxide nanoparticles using *Carica papaya* leaf extract through a green, environmentally friendly method. Characterization results confirmed the formation of functional and structurally stable nanoparticles with suitable properties for environmental application. The synthesized CuO nanoparticles demonstrated effective adsorption capacity in removing hardness from naturally polluted surface water, with removal efficiencies generally improving with nanoparticle dosage and favorable physicochemical conditions

References

Abdelmonem, B. H., Kamal, L. T., Elbaz, R. M., Khalifa, M. R., & Abdelnaser, A. (2025). From contamination to detection: The growing threat of heavy metals. *Heliyon, 11*(1).

Alfaifi, A. H., Alkhattaby, L. A., El-Qahtani, Z. M., Al-Ghamdi, W., Althobaiti, H. A., Al-Balawi, S., . . . Rajeh, A. (2025). An insight into the influence of CuO NPs on the structural, dielectric, optical, and conductivity properties of PEO/PVA-CuO nanocomposite for energy storage nanoelectronic devices. *Emergent Materials, 8*(1), 263–277.

Baral, J., Pokharel, N., Dhungana, S., Tiwari, L., Khadka, D., Pokhrel, M. R., & Poudel, B. R. (2025). Green synthesis of copper oxide nanoparticles using Mentha (mint) leaves characterization and its antimicrobial properties with phytochemicals screening. *Journal of Nepal Chemical Society, 45*(1), 111–121.

Boddu, S., Marri, B. P., Katika, R. M., Mikkili, I., Dulla, J. B., Allugunulla, V. N., . . . Khan, A. A. (2025). Green synthesis of copper oxide nanoparticles (CuONPs) using Ricinus communis: Efficient photocatalytic dye degradation and antibacterial applications. *Water, Air, & Soil Pollution, 236*(4), Article 209.

Dhoke, S. K. (2025). Determination of total hardness of water sample by titration using double burette method: An economical approach. *Chemistry Teacher International, 7*(3), 545–552.

Ezeoke, C. H., Sadiq, Z., Safiabadi Tali, S. H., & Jahanshahi-Anbuhi, S. (2025). Reverse titration using tablets for accurate water hardness measurement with improved resistance to interference. *Chemosensors, 13*(10), Article 365.

Gaddigal, A. T., Shivappa, P., Ganeshkar, M. P., Mirjankar, M. R., Poojari, P. B., Huyilagola, P. V., . . . Kamanavalli, C. M. (2025). Green synthesis of copper oxide nanoparticles using Simarouba glauca leaf extract, characterization and screening for their biological applications. *Journal of Dispersion Science and Technology, 46*(12), 1916–1930.

Ge, Y., Wang, W.-M., & Liu, T. (2025). An isothermal titration calorimetry method for monitoring the removal of ethylenediamine tetra-acetic acid from apo-proteins. *Results in Chemistry, 16*, Article 102373.

Hadkar, V. M., & Selvaraj, C. I. (2025). Characterization and investigating the potential therapeutic effects of phyto-assisted CuO and Zn-doped CuO nanoparticles from Calophyllum apetalum (Willd.) leaf extract. *Journal of Drug Delivery Science and Technology, 104*, Article 106530.

Joolaei Ahranjani, P., Dehghan, K., Esfandiari, Z., & Joolaei Ahranjani, P. (2025). A systematic review of spectroscopic techniques for detecting milk adulteration. *Critical Reviews in Analytical Chemistry*, 1–32. Advance online publication.

Kalaiyan, G., Topare, N. S., Sikiru, S., Thambidurai, S., Kandasamy, M., Pugazhenthiran, N., . . . Suresh, S. (2025). Green synthesis of copper oxide nanoparticles using Euphorbia heterophylla leaf extract for deactivation of pathogenic bacteria and photocatalytic degradation of industrial dyes. *Results in Engineering, 26*, Article 104797.

Kalesh, K. N., & Vadhavaniya, S. (2025). Modern trends in volumetric analysis: A comprehensive review of redox, complexometric and diazotization titrations in drug estimation. *Journal of Advance and Future Research, 3*(11), 107–124.

Manimehala, U., Asha, S., Tomy, M., Anu, M., Sumitha, M., Kumar, P., . . . Binoy, J. (2025). Green synthesis of copper oxide nanoparticles from Camellia sinensis extract: Effects of calcination temperatures on antimicrobial activity. *Biochemical and Biophysical Research Communications, 769*, Article 151963.

Moroda, M. D., Deressa, T. L., Tiwikrama, A. H., & Chala, T. F. (2025). Green synthesis of copper oxide nanoparticles using Rosmarinus officinalis leaf extract and evaluation of its antimicrobial activity. *Next Materials, 7*, Article 100337.

Rogóż, W., Owczarzy, A., Kulig, K., & Maciążek-Jurczyk, M. (2025). Ligand-human serum albumin analysis: The near-UV CD and UV-Vis spectroscopic studies. *Naunyn-Schmiedeberg's Archives of Pharmacology, 398*(3), 3119–3131.

Selim, H. M. R. M., Saleh, A., Soliman, N. R., Abdelkhalig, S. M., Mattar, E., Mahmoud, M. M., . . . Hamed, A. A. (2025). Myco-fabricated CuO NPs and chitosan-conjugated CuO nanoparticles using endophytic Aspergillus sp. JAWF3: Targeting E. coli outer membrane for enhanced antibacterial and biofilm inhibition. *Inorganic Chemistry Communications, 178*, Article 114361.

Singh, A. V., Bansod, G., Schumann, A., Bierkandt, F. S., Laux, P., Nakhale, S. V., . . . Luch, A. (2025). Investigating tattoo pigments composition with UV-Vis and FT-IR spectroscopy supported by chemometric modelling. *Current Analytical Chemistry, 21*(8), 988–1004.

Swarna, S., Govindarajan, V. U., Anbalagan, A., Christopher, D., & Muthuraman, M. S. (2025). Green synthesis of copper oxide nanoparticles using Ziziphus oenoplia extract and its dye degradation properties. *Biomass Conversion and Biorefinery, 15*(19), 26725–26736.

Veg, E., Raza, A., Rai, S., Sharma, S., Pandey, A., Imran Ahmad, M., . . . Khan, T. (2025). Synthesis, characterization and antibacterial activity evaluation of CuO NPs and B-CuO NPs obtained from Livistona chinensis leaf extract. *Chemistry & Biodiversity, 22*(2), Article e202401596.

Acknowledgements

The authors are deeply appreciative of the invaluable assistance given by Mal. Ya,u (Laboratory Unit, Federal University Dutse) and Dr. N. Mansir (HOD, Department of Chemistry, Federal University Dutse) regarding sample preparation and analysis.